

1
2
3
4
5
6
7
8
9
10
11
12
13
14
15
16
17
18
19

Lead pollution of coastal sediments by ceramic waste

Andrew Turner*

*School of Geography, Earth and Environmental Sciences, University of Plymouth, Drake
Circus, Plymouth PL4 8AA, UK*

*Corresponding author

e-mail: aturner@plymouth.ac.uk

<https://doi.org/10.1016/j.marpolbul.2018.11.013>

Accepted 8th November 2018

Embargoed until 8th November 2020

20 **Abstract**

21 Ceramic fragments and fractionated (< 2 mm) sediment have been sampled from two
22 beaches in southwest England, along with sediment from a control beach where ceramic
23 waste was lacking. Analysis of the glazed ceramic surfaces by X-ray fluorescence (XRF)
24 spectrometry returned concentrations of Pb up to 729,000 mg kg⁻¹, while XRF analysis of
25 sediment samples revealed high but heterogeneous concentrations of Pb at the two sites
26 impacted by ceramic waste (median = 292 and 737 mg kg⁻¹) compared with the control
27 beach (median ~ 20 mg kg⁻¹). These observations are attributed to the disposal of
28 contemporary and historical ceramic products, and the subsequent attrition of material and
29 contamination of local sediment. Extraction of a milled ceramic composite (Pb = 2780 mg
30 kg⁻¹) by 1M HCl, revealed a high (34%) environmental mobility and availability of Pb;
31 extraction in a solution of protein, however, suggested a low (0.1%) bioaccessibility to
32 sediment-ingesting invertebrates.

33

34 **Keywords:**

35 Ceramic fragments; glaze; lead; sediments; contamination

36

37

38

39

40

41

42

43

44

45

46 **1. Introduction**

47 Heavy metals enter rivers, estuaries and coastal waters through natural erosion in the
48 catchment and from a variety of anthropogenic sources, including municipal and industrial
49 waste, stormwater, metal mining and processing, boating and shipping activities and
50 agriculture (Cave et al., 2005; Pan and Wang, 2012). Sediment is the principal receptacle of
51 metals in these environments, mainly because its high surface area and chemical reactivity
52 allow charged species to readily undergo exchange reactions, adsorption and co-precipitation
53 at the particle surface (Turner and Millward, 2002). Metals may also be present in sediment
54 when associated with discrete, contaminated particulates, like fly ash, paint fragments, tyre-
55 wear particles and microplastics (Pratt and Lottermoser, 2007; Massos and Turner, 2017)
56 which, in some instances, make a significant contribution to overall metal loading. For
57 example, tyre wear particles enriched in Zn, which serves as an activator or accelerator for
58 the rubber vulcanization process, may contribute up to 10% of the sedimentary reservoir in
59 the vicinity of major highways (Voparil et al., 2004), while antifouling paint fragments
60 containing high levels of Cu as a biocide make considerable contributions to the sediment
61 loading in the vicinity of boat repair facilities (Singh and Turner, 2009).

62

63 While measuring heavy metals in intertidal sediments from the Tamar estuary, southwest
64 England, using a portable X-ray fluorescence (XRF) spectrometer (Turner and Taylor,
65 2018), we noted elevated concentrations of Pb at various locations towards the estuary
66 mouth. At one site, concentrations of Pb, but not other metals, were an order of magnitude
67 higher than concentrations in the upper catchment that is impacted heavily by historic
68 mining activities. Sediments at this site were coarse (sand-gravel-pebble) compared with the
69 fine silts of the upper catchment but were characterised by an abundance of visible fragments
70 of ceramic debris that were usually off-white or brown but occasionally brightly-coloured.
71 Subsequent inspection of other beaches in the region revealed that ceramic debris was

72 commonly present where sediment was relatively coarse, especially towards the high water
73 line. Since lead oxide was (and, in some cases, still is) employed as a flux in the glazing of
74 ceramics (Beldi et al., 2016), it is hypothesized that the presence and attrition of such
75 material may act as a significant source of local Pb contamination.

76

77 In this study, sediments and glazed ceramics have been collected from two beaches in the
78 Plymouth Sound region of southwest England and analysed directly and non-destructively
79 for Pb using XRF; an additional beach with little ceramic waste evident was sampled for
80 sediment as a control. In order to evaluate the mobility and environmental significance of Pb
81 from this source, a composite of glazed ceramics was prepared by milling and subjected to
82 XRF analysis and to different chemical treatments, with extracts analysed by conventional
83 inductively coupled plasma techniques.

84

85

86 **2. Materials and methods**

87 *2.1. Study sites*

88 Plymouth Sound, south west England is an open, macrotidal bay facing the English Channel
89 whose inner waters are up to 40 m deep and are sheltered by a 1600 m breakwater. The
90 coastline is steeply sloping and rocky, with numerous small coves and beaches. The Tamar
91 and Plym estuaries enter the Sound from the north west and north east, respectively, and
92 supply the majority of freshwater to the system. The inner Sound and lower estuaries are
93 urbanised and support a number of maritime, shipping, naval and fishing industries as well
94 as various water sports.

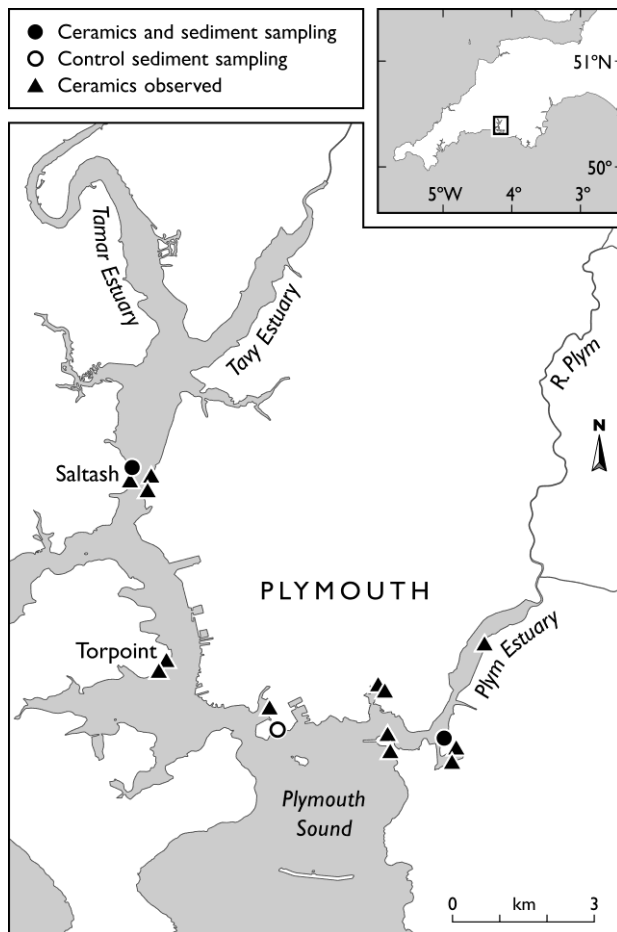
95

96 *2.2. Sampling*

97 Samples were collected during March and September of 2017 from three sand-gravel-pebble
98 beaches around the coastal zone of Plymouth and at the locations shown in Figure 1;
99 specifically, at Oreston on the lower Plym estuary, Saltash on the lower Tamar estuary, and
100 Firestone Bay in Plymouth Sound. Previous visits to a number of sites and counting with 0.5
101 m² quadrats had revealed that ceramic fragments were most abundant at the former two
102 locations, especially in the upper reaches of the intertidal zone, while the latter location was
103 relatively free of such material.

104

105 Three surficial (< 1 cm) intertidal sediment samples of about 200 g were collected using a
106 plastic spatula at three sites from each location that were approximately 20 m apart. Samples
107 were returned to the laboratory in resealable polyethylene bags where they were oven-dried
108 in open crucibles at 40 °C overnight. Dried samples were then sieved through a 2 mm nylon
109 mesh and the fine fraction transferred to new polyethylene bags. Fragments of ceramics that
110 were clearly visible to the naked eye were collected manually from a 1 m² quadrat centred on
111 the sediment sample sites and counted into a series of polyethylene bags. In the laboratory,
112 ceramics were cleaned with a nylon brush under running water and dried as above before
113 being stored in air-tight polyethylene boxes.



114

115 **Figure 1: Locations for sampling and where ceramic waste was observed in the**
 116 **Plymouth Sound region of southwest England.**

117

118 *2.3. Sediment analysis*

119 Sediments were analysed directly in their bags and at six different positions through the face
 120 of each polyethylene sample bag using a Niton XL3t 950 He GOLDD+ portable XRF
 121 housed in a 4000 cm³ laboratory accessory stand. Measurements for Pb and a suite of other
 122 metals whose fluorescent energies were not significantly attenuated by polyethylene (Bi, Cu,
 123 Rb, Sb, Sn, Zn) were conducted in a ‘mining’ mode and with a beam width of 8 mm
 124 (equivalent to a measurement area of 50 mm²) for a total time of 60 s, comprising successive
 125 counting periods of 30 s at 50 kV/40 μA (main filter), 15 s at 20 kV/100 μA (low filter) and
 126 15 s at 50 kV/40 μA (high filter). Spectra arising from sample counting were quantified by

127 fundamental parameter coefficients to yield metal concentrations in mg kg^{-1} and with a
128 measurement counting error of 2σ (95% confidence).

129

130 The detection limit for Pb in sediment, based on errors arising from samples returning the
131 lowest concentrations, was around 9 mg kg^{-1} . Multiple analyses of a reference sediment
132 (GBW07318) that had been packed into a polyethylene XRF sample cup (Chemplex series
133 1400, 21-mm internal diameter) and collar-sealed with $3.6 \mu\text{m}$ SpectraCertified Mylar
134 polyester film returned concentrations of Pb, Cu and Zn that were within 15 % of certified
135 values (66 ± 6 , 66 ± 7 and $165\pm 15 \text{ mg kg}^{-1}$, respectively).

136

137 *2.4. Ceramic analysis*

138 Selected ceramic samples were analysed by XRF in a 'plastics' mode and a 'lead paint'
139 mode. In the plastics mode, a thickness correction of 0.05 mm was applied that accounted for
140 the film-like characteristics of the glaze. The central area of the glazed surface was measured
141 (and on both internal and external surfaces where possible) for Pb with a beam width of 8
142 mm and for a total time of 60 s, comprising successive counting periods of 40 s with the
143 main filter and 20 s with the low filter. Concentrations were returned by fundamental
144 parameters in mg kg^{-1} with a detection limit, as defined above, of about 6 mg kg^{-1} . Where the
145 surface was patterned or multi-coloured, different areas were probed by moving the sample
146 with respect to the detector window, a process aided by live imagery generated by the CCD
147 camera adjacent to the x-ray source. Samples of different colour, condition and Pb
148 concentration were also analysed by XRF in a lead paint mode. Here, the instrument was
149 operated at 8 mm and for a counting period of 30 s at 50 kV and $40 \mu\text{A}$, and returned
150 concentrations of Pb through fundamental parameters in mg cm^{-2} . Concentrations of Pb
151 determined in six standard reference paint films (SRM 2570 to 2575; National Institute of
152 Standards & Technology) were within 15% of corresponding certified values.

153

154 *2.5. Ceramic composite*

155 A fine, working composite sample of ceramics, representing aged (eroded and abraded)
156 material, was prepared from various fragments of different visual and chemical
157 characteristics. Thus, six fragments from Oreston and six from Saltash were crushed into a
158 powder in a tungsten bowl at 700 rpm for 30 s and 1400 rpm for 20 s using a Retsch RS100
159 puck mill. The powder was transferred into two separate resealable polyethylene bags under
160 a dust extractor, with one bag analysed directly by XRF in its mining mode as above and
161 material in the second bag used in the extraction tests described below.

162

163 *2.6. Extraction tests*

164 The powdered composite was subject to extraction in cold 1 M HCl (Fisher Scientific Trace
165 analysis grade) and 5 g L⁻¹ bovine serum albumin (BSA; >96% fraction V, Sigma Aldrich)
166 The former extract is designed as a simple means of evaluating the general mobility or
167 bioavailability of heavy metals and is often used in the first tier of sediment quality
168 assessment (McCready et al., 2003), while the latter extract provides a more specific
169 estimation of metal bioaccessibility to deposit-feeding invertebrates (Kalman and Turner,
170 2007). Thus, three 1 g portions of the composite were weighed into individual 100 ml acid-
171 cleaned Pyrex beakers and 50 ml of 1 M HCl added. The contents, plus three beakers
172 containing acid and no solids, were left at room temperature with occasional agitation for a
173 period of 6 h before being filtered through Whatman 0.45 µm filters into individual 60 ml
174 polypropylene centrifuge tubes. This process, including corresponding controls, was
175 repeated using BSA solution in place of HCl.

176

177 *2.7. Extract analyses*

178 Concentrations of Pb in the HCl-extracts of the milled composite were determined by
179 inductively coupled plasma-optical emission spectrometry (ICP-OES) using a Thermo
180 Scientific iCAP 7400 analyser with a MiraMist PEEK nebuliser and cyclonic spray chamber.
181 The instrument was calibrated using four matrix-matched standards in the range 0.2 to 20 mg
182 L⁻¹ and a matrix-matched blank. Instrument RF power was set at 1.2 KW, coolant, auxiliary
183 and nebuliser flows were 12, 0.5 and 0.5 L Ar min⁻¹, respectively, and replicate ($n = 3$) read
184 time was 2 s. Lead concentrations in the BSA-extracts were determined by inductively
185 coupled plasma-mass spectrometry (ICP-MS) using a Thermo Scientific iCAP RQ analyser
186 with a Glass Expansion micromist nebuliser and cyclonic spray chamber. The instrument
187 was calibrated with a blank and three matrix-matched standards in the range 10 to 100 µg L⁻¹,
188 and RF power was set at 1.5 KW with coolant, nebuliser and auxiliary flows of 1.4, 1.07
189 and 0.8 L Ar min⁻¹ and a replicate ($n = 3$) read time of 10 ms.

190

191 **3. Results**

192 *3.1. Characteristics of the ceramic samples*

193 Ceramic fragments were abundant amongst the sand-gravel-pebbles of the upper intertidal
194 zones of Oreston and Saltash, with up to several hundred pieces per m² visible at the surface
195 where counting had been performed. Fragments were evident at many other locations in the
196 region (Figure 1), with abundance greater in more sheltered embayments than on beaches
197 facing directly on to Plymouth Sound. In total, 48 ceramic samples were analysed from
198 Oreston and 24 fragments were analysed from Saltash, with a selection of samples illustrated
199 in Figure 2. Samples were an heterogeneous assortment of rounded or angular fragments of
200 earthenware, stoneware and porcelain of different sizes, colours and degrees of aging.



201

202 **Figure 2:** A selection of ceramic fragments retrieved from Oreston and Saltash and
203 presented on cm-scaled paper.

204

205 The primary length of most fragments ranged from about 2 to 5 cm, with thicknesses usually
206 around 3-6 mm but that exceeded 1 cm in isolated cases and masses that varied between
207 about 2 and 20 g. Most samples exhibited an inherent curvature and glazing on both
208 surfaces, with many fragments having a distinctive lip or base area and a few fragments
209 characterised by a ribbed or ridged surface; other samples, however, were flat and often
210 unglazed on one side. The décor below glazed surfaces was most commonly white to off-
211 white or brown-beige, with blue-green and yellow fragments also present, while the paste of
212 most samples was off-white or brown. A few samples were decorated in different colours
213 and lipped areas were occasionally coloured differently to the main, curved surfaces. The
214 glazing of some ceramics appeared to be in relatively good condition but the majority of

215 samples exhibited various degrees of crazing. Other evidence of aging and erosion was the
216 presence of cracks and pits on the surface, areas where the glazing and décor had been
217 completely dislodged from the underlying ceramic body, and regions of inorganic fouling
218 and algal growth.

219

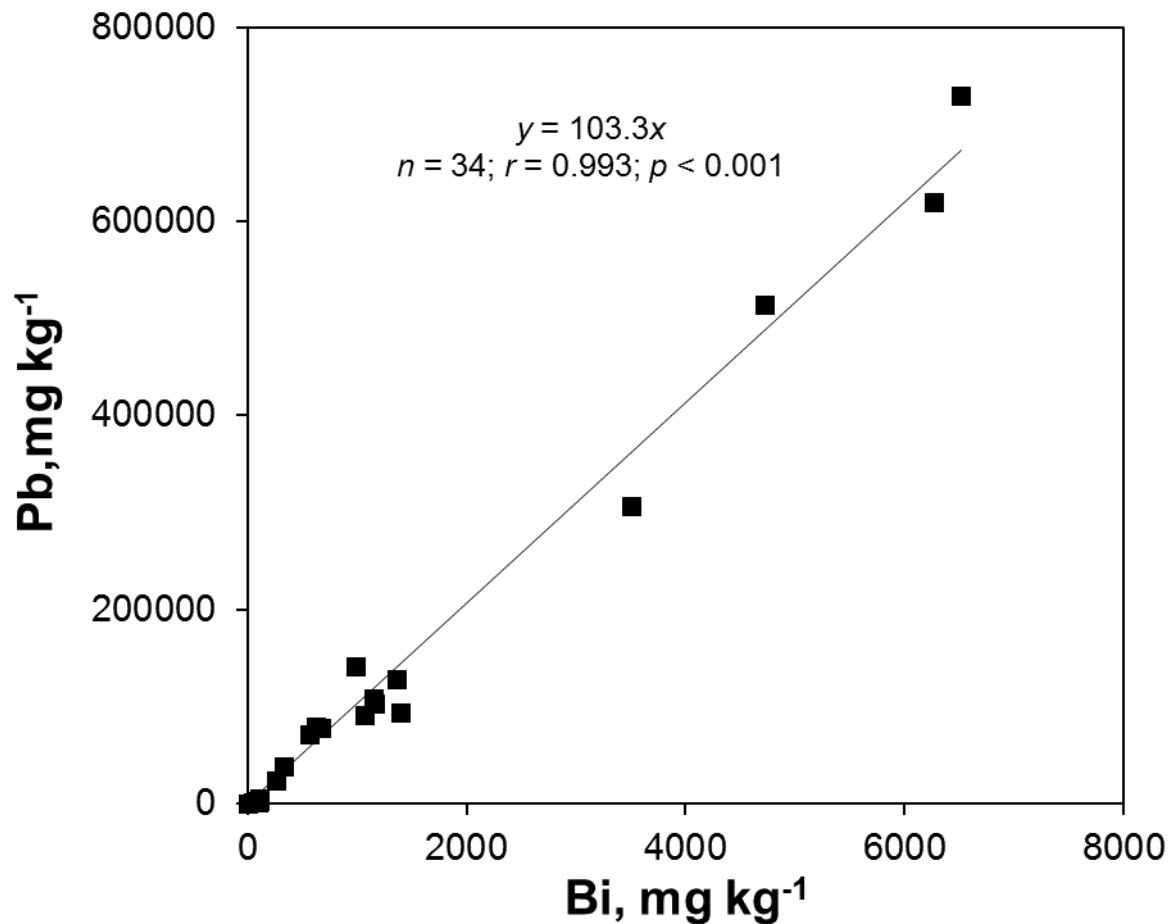
220 *3.2. Lead concentrations in the ceramic samples*

221 Concentrations of Pb in the glazed surfaces of the ceramic samples from Oreston and Saltash
222 that had been analysed by XRF are summarised in Table 1. Here, concentrations are based
223 on single measurements performed in the centre of the outer surface. Note that multiple
224 measurements over a reasonably uniform surface returned concentrations with a relative
225 standard deviation of < 20% and that measurements of inner surfaces were often constrained
226 by accessibility or distance to the XRF detector window. Lead was detected in all 24 samples
227 analysed from Saltash and in 45 out of 48 samples analysed from Oreston, with
228 concentrations that were highly variable and that, overall, ranged from < 10 mg kg⁻¹ to about
229 70% by weight. There was no clear relationship between Pb concentration and sample
230 thickness, curvature or décor colour but concentrations below 100 mg kg⁻¹ were usually
231 encountered in samples that appeared to be relatively clean, angular and new.

232

233 Other heavy metals (and metalloids) that were detected by the XRF in many (but not all)
234 ceramic samples analysed included Bi, Cu, Sb, Sn and Zn and with median concentrations of
235 451, 62, 563, 1160 and 296 mg kg⁻¹, respectively. While the concentrations of the latter
236 elements exhibited no clear co-association with concentrations of Pb, concentrations of Bi
237 (where detected) and Pb exhibited a striking and highly significant linear relationship that is
238 shown in Figure 3.

239



240

241 Figure 3: Concentrations of Pb versus concentrations of Bi in the ceramic fragments.

242

243 Lead was also measured in selected samples ($n = 15$) on an areal basis using a lead paint
 244 mode and with units of mg cm^{-2} that are consistent with many Pb-based paint assessments
 245 and regulations (Clark et al., 2006). The concentrations arising from this approach ranged
 246 from 0.03 to 23.1 mg cm^{-2} and were highly correlated with concentrations determined in
 247 plastics mode and in mg kg^{-1} ($r = 0.989$; $p < 0.001$), with a best-fit linear regression line
 248 defining the data of $y = 29,900x$, or a conversion factor between the two measures of 29.9
 249 $\text{cm}^2 \text{g}^{-1}$. The lead paint mode also returns a depth index that provides a semi-quantitative
 250 evaluation of the depth of the layer of Pb. An average value of 1.5 and no values above 2 for
 251 the samples tested confirms that the metal is located at or near the surface of the ceramics.

252
 253
 254
 255
 256
 257
 258
 259
 260
 261
 262
 263
 264
 265
 266
 267
 268
 269
 270
 271
 272
 273
 274
 275

Table 1: Frequency distribution and summary statistics for Pb concentrations (in mg kg⁻¹) in the glazed surfaces of ceramic samples from Oreston and Saltash.

	< 10 ²	10 ² -10 ³	10 ³ -10 ⁴	10 ⁴ -10 ⁵	>10 ⁵	mean	median	min	max
Oreston (n = 48)	6	10	5	22	5	45,000	29,300	79.0	402,000
Saltash (n = 24)	4	4	3	6	7	121,000	29,900	9.3	729,000

3.3. Lead concentrations in the ceramic composite and release by HCl and BSA

The concentration of Pb in the ceramic composite prepared by milling 12 individual fragments and determined by XRF in mining mode was 2780 ± 286 mg kg⁻¹ (n = 6). Other heavy metals were detected but at significantly lower concentrations; specifically, concentrations of Bi, Sn and Zn were 36.7 ± 6.2, 46.5 ± 11.7 and 477 ± 62 mg kg⁻¹, respectively, and Cu was undetected. Lead mobilised by 1M HCl and determined by ICP was 953 ± 91.6 mg kg⁻¹, or 34% of total Pb determined by XRF, while the corresponding values mobilised by 5 g BSA L⁻¹ were 2.5 ± 0.86 mg kg⁻¹ and 0.1%.

3.3. Lead concentrations in the sediment samples

Concentrations of Pb in the three fractionated (< 2 mm) sediments taken from each location and measured at six different positions through the face of the polyethylene bag are summarised in Table 2. At the control location (Firestone Bay), mean concentrations are similar among the three samples and, overall, concentrations range from about 11 to 30 mg kg⁻¹. At the locations impacted by ceramic waste, both mean and individual concentrations of Pb are more variable, with concentrations ranging from about 80 to 1400 mg kg⁻¹ at Oreston and 310 to 1000 mg kg⁻¹ at Saltash. On average, Pb concentrations at these locations are greater than the control location by factors of 20 or more.

276 In order to account for granular and mineralogical variations among the sediment samples,
277 Pb data were normalised with respect to a geochemical proxy. While Al or Fe are
278 conventionally employed as proxies (Schiff and Weisberg, 1999; Ho et al., 2012), the
279 fluorescent energies of the former are too low to be analysed by portable XRF in air and the
280 region is impacted by high and variable concentrations of the latter through acid mine
281 drainage in the upper Tamar catchment (Mighanetara et al., 2009). Accordingly, Rb was
282 selected as a normaliser because of its propensity to substitute for K in fine-grained clays
283 and its ready determination by XRF (Rae, 1995; Lewis and Turner, 2018). Concentrations of
284 Rb, shown in Table 2, reveal relatively invariant concentrations within the same sample and
285 between samples taken from the same site, suggesting that local variations in Pb
286 concentration are not the result of variations in sediment granulometry but are the result of
287 heterogeneous contamination. Variations in Rb concentration between locations, however,
288 suggest that grain size varies across the region; specifically, higher concentrations at Oreston
289 and Saltash than Firestone suggest a finer distribution of material at the former locations.

290

291 Rubidium-normalised Pb concentrations were used to compute mean enrichment factors, EF,
292 for sediments at Oreston and Saltash as follows:

293

$$294 \quad EF = ([Pb]/[Rb])/([Pb]_b/[Rb]_b)^{-1}$$

295

296 where the denominator represents baseline Rb-normalised Pb concentrations that are derived
297 from mean concentrations of the metals at Firestone Bay. Values of EF exceeding unity,
298 shown in Table 2, confirm that the locations impacted by ceramic waste are contaminated by
299 Pb, with the extent of Pb contamination ranging from about 5.4 for one sediment at Oreston
300 to over 13 for a sample from Saltash.

301

302 **Table 2:** Summary statistics for Pb concentrations and mean concentrations of Rb in the
 303 three < 2 mm sediment samples from each location that were analysed at six different
 304 positions through the face of the polyethylene bag. EF denotes mean enrichment factors for
 305 Pb based on normalisation with respect to Rb.

				Pb		Rb	EF
		mean+1 sd	median	min	max	mean+1 sd	
Firestone Bay	(i)	19.5 _{+8.3}	15.1	11.4	30.1	50.3 _{+9.2}	
	(ii)	21.0 _{+5.2}	22.3	14.5	28.3	47.5 _{+3.3}	
	(iii)	20.9 _{+6.3}	22.0	11.4	28.3	48.6 _{+6.7}	
Oreston	(i)	414 ₊₄₈₈	292	81.3	1390	180 _{+27.7}	5.35
	(ii)	564 ₊₂₅₆	485	304	987	165 _{+23.8}	7.95
	(iii)	501 ₊₁₉₀	425	307	804	168 _{+11.4}	6.93
Saltash	(i)	518 ₊₁₈₁	461	370	872	146 _{+8.1}	8.25
	(ii)	481 ₊₁₁₉	467	307	660	144 _{+22.8}	7.77
	(iii)	751 ₊₁₇₂	737	570	1010	133 _{+18.7}	13.13

306

307

308 **4. Discussion**

309 While OSPAR (2010) includes ceramics in their categorisation of marine litter, only a
 310 handful of studies appear to have referred to this type of waste while classifying beached
 311 materials (Ioakeimidis et al., 2014; Buhl-Mortensen and Buhl-Mortensen, 2016). The results
 312 of this study are, therefore, significant in revealing the extent of heterogeneous
 313 contamination by ceramic debris that is possible in the intertidal zone. Although quantitative
 314 analysis was restricted to two beaches around Plymouth Sound, inspections of other local
 315 beaches revealed varying degrees of contamination in many other cases (Figure 1), with
 316 accumulations most often observed among gravel-pebble deposits of the upper intertidal
 317 zone but also apparent on fine, intertidal mudflats. Clearly, it is likely that other
 318 environments of similar (historic) usage and setting are subject to comparable contamination
 319 by ceramic debris.

320

321 Potential sources of ceramics to the region under study include historic landfill sites and
322 various construction projects and manufacturing industries. However, fragments typical of
323 those sampled would be too large and dense to be transported and redistributed across
324 Plymouth Sound, suggesting that sources are more localised. That ceramic debris was more
325 abundant in the vicinity of informal boating activities (repair, maintenance and renovation)
326 implies material may be partly derived from the disposal and fragmentation of shipboard
327 sanitary equipment and tiles. This practice may also attract the tipping of additional
328 municipal wastes, including crockery and garden ceramics, in the immediate vicinity (Turner
329 and Rees, 2016), with lighter material like plastics, ropes and foams more readily swept
330 away or recognised and collected as litter. More generally, however, it is suspected that
331 material has accumulated in the intertidal zone over extended periods of time (centuries)
332 through the historic use of utilitarian and, later, decorated products for the storage,
333 transportation and trading of a wide range of goods, including food, wine, chemicals and
334 molasses. Because of their natural colours, these fragments blend into the sand-gravel-pebble
335 substrate and have, therefore, evaded collection and disposal as waste.

336

337 The majority of the ceramic fragments retrieved in the present study were glazed, with
338 surfaces that were usually characterised by high concentrations of Pb. This observation is
339 consistent with the pervasive use of lead oxide (PbO) as a flux of low melting point, wide
340 firing range and high refractive index. Other oxides that were evident in some of the samples
341 and that co-existed with high concentrations of Pb included those of Sn and Zn. However,
342 the striking correlation of Bi with Pb suggests that bismuth trioxide (Bi_2O_3) has been used
343 extensively as a component of ceramic fluxes in tandem with PbO (and at a mass ratio of
344 Pb:Bi of about 100).

345

346 High concentrations of Pb in the glaze affords the potential for heterogeneous contamination
347 of local sediment as the ceramics break down through weathering and abrasion; this is
348 reflected by high (but variable) EF values at Oreston and Saltash for sediments fractionated
349 to < 2 mm. It is unclear how thick the glazed layer of the ceramics is but the Pb
350 concentration of the milled composite of 2800 mg kg⁻¹ is assumed to be a representative
351 value for the bulk material (that includes the paste) as a contaminant. Thus, assuming a
352 background sediment concentration of Pb for the region of 20 mg kg⁻¹ based on results for
353 the control location and a sediment concentration of 400 mg kg⁻¹ representative of sites
354 contaminated by ceramic debris, mass balance requires that, on average, ceramic-derived
355 material contributes about 14% to the total mass of (< 2 mm) sediment in contaminated
356 settings.

357

358 The mobility or general availability of Pb in the milled composite of ceramics was evaluated
359 using cold 1M HCl. With respect to estuarine and coastal sediments, this fraction is often
360 assumed to represent metal bound in non-residual fractions and where the majority of
361 anthropogenic metals reside, as well as providing a general proxy for monitoring the
362 bioavailability and biological effects of heavy metals (Riddle et al., 2003; Bettiol et al.,
363 2008). While the percentage of total Pb mobilised from the ceramic composite (around 34%)
364 is lower than that typically mobilised from contaminated sediments (in excess of 80% has
365 been reported; McCready et al., 2003), it is nevertheless significant and indicates that the
366 weathered and eroded glaze of ceramics may be an important source of mobile Pb in coastal
367 sediments impacted by visible debris. In contrast, however, the availability of Pb in the
368 composite to the protein, BSA, is only about 0.1% of its total content and is considerably
369 lower than the percentage mobilised in contaminated sediment (around 10%; Kalman and
370 Turner, 2007). Thus, despite its high mobility under acidic conditions, Pb in ceramic debris

371 is not predicted to be particularly accessible in non-acidic digestive conditions typical of
372 sediment-feeding invertebrates or under near-neutral aqueous conditions more generally.

373

374 **5. Conclusions**

375 This study has highlighted the potential significance of glazed surfaces as a source of Pb to
376 estuarine and coastal sediments that are visibly impacted by ceramic wastes. At the sites
377 under investigation, the presence of glazed ceramics that have been eroded to sizes < 2 mm
378 result in increases in Pb concentrations relative to a regional baseline of about an order of
379 magnitude and enrichment factors normalised to Rb of between 5 and 13. Lead arising from
380 glazed ceramic surfaces has a mobility of more than 30% as evaluated by extraction in cold
381 HCl, but is unlikely to be assimilated by deposit-feeding invertebrates because of its poor
382 solubility in a surrogate digestive protein. While the specific findings of the study are
383 localised, it would be reasonable to assume that the broad impacts documented are more
384 generally applicable where ceramic waste is observed.

385

386 **Acknowledgements**

387 This study was partly funded by a HEIF Plymouth University Marine Institute grant. Dr
388 Andy Fisher and Mr Ben Lowe are thanked for assistance with the preparation and analysis
389 of the ceramic extracts.

390

391 **References**

392 Beldi, G., Jakubowska, N., Peltzer, M.A., Simoneau, C., 2016. Testing approaches for the
393 release of metals from ceramic articles: In support of the revision of the
394 Ceramic Directive 84/500/EEC. Publications Office of the European Union, Luxembourg,
395 86pp.

396

397 Bettiol, C., Stievano, L., Bertelle, M., Delfino, F., Argese, E., 2008. Evaluation of
398 microwave-assisted acid extraction procedures for the determination of metal content and
399 potential bioavailability in sediments. *Applied Geochemistry* 23, 1140-1151.
400

401 Buhl-Mortensen, L., Buhl-Mortensen, P., 2016. Marine litter in the Nordic Seas: Distribution
402 composition and abundance. *Marine Pollution Bulletin* 125, 260-270.
403

404 Cave, R.R., Andrews, J.E., Jickells, T., Coombes, E.G., 2005. A review of sediment
405 contamination by trace metals in the Humber catchment and estuary, and the implications
406 for future estuary water quality. *Estuarine, Coastal and Shelf Science* 62, 547-557.
407

408 Clark, C.S., Rampal, K.G., Thuppil, V., Chen, C.K., Clark, R., Roda, S., 2006. The lead
409 content of currently available new residential paint in several Asian countries.
410 *Environmental Research* 102, 9-12.
411

412 Ho, H.H., Swennen, R., Cappuyns, V., Vassilieva, E., Van Tran, T., 2012. Necessity of
413 normalization to aluminum to assess the contamination by heavy metals and arsenic in
414 sediments near Haiphong Harbor, Vietnam. *Journal of Asian Earth Sciences* 56, 229-239.
415

416 Ioakeimidis, C., Zeri, C., Kaberi, H., Galatchi, M., Antoniadis, K., Streftaris, N., Galgani,
417 N., Papathanassiou, E., Papatheodorou, G., 2014. A comparative study of marine litter on the
418 seafloor of coastal areas in the Eastern Mediterranean and Black Seas *Marine Pollution*
419 *Bulletin* 89, 296-304.
420

421 Kalman, J., Turner, A., 2007. An evaluation of metal bioaccessibility in estuarine sediments
422 using the commercially available protein, bovine serum albumin. *Marine Chemistry* 107,
423 486-497.

424

425 Massos, A., Turner, A., 2017. Cadmium, lead and bromine in beached microplastics.
426 *Environmental Pollution* 227, 139-145.

427

428 McCready, S., Birch, G.F., Taylor, S.E., 2003. Extraction of heavy metals in Sydney
429 Harbour sediments using 1M HCl and 0.05M EDTA and implications for sediment-quality
430 guidelines. *Australian Journal of Earth Sciences* 50, 249-255.

431

432 Mighanetara, K., Braungardt, C.B., Rieuwerts, J.S., Azizi, F., 2009. Contaminant fluxes
433 from point and diffuse sources from abandoned mines in the River Tamar catchment, UK.
434 *Journal of Geochemical Exploration* 100, 116-124.

435

436 OSPAR Commission, 2010. Guideline for monitoring marine litter on the beaches in the
437 OSPAR maritime area. OSPAR Commission, London, 84pp.

438

439 Pan, K., Wang, W.X., 2012. Trace metal contamination in estuarine and coastal
440 environments in China. *Science of the Total Environment* 421, 3-16.

441

442 Pratt, C., Lottermoser, B.G., 2007. Mobilisation of traffic-derived trace metals from road
443 corridors into coastal stream and estuarine sediments, Cairns, northern Australia.
444 *Environmental Geology* 52, 437-448.

445

446 Rae, J.E., 1997. Trace metals in deposited intertidal sediments. In: Biogeochemistry of
447 Intertidal Sediments, ed. T.D. Jickells and J.E. Rae, Cambridge University Press, pp.16-41.
448

449 Riddle, M.J., Scouller, R.C., Snape, I., Stark, J.S., Kratzmann, S.M., Stark, S.C., King, C.K.,
450 Duquesne, S., Gore, D.B., 2003. From chemical monitoring to biological meaning:
451 extraction techniques and the biological interpretation of sediment chemistry data from the
452 Casey region. Antarctic Biology in a Global Context, Proceedings, Edited by: Huiskes,
453 A.H.L., Gieskes, W.W.C., Rozema, J., Schorno, R.M.L., Van Der Vies, S.M., Wolff, W.J.,
454 pp 285-289.
455

456 Schiff, K.C., Weisberg, S.B., 1999. Iron as a reference element for determining trace metal
457 enrichment in Southern California coastal shelf sediments. Marine Environmental Research
458 48, 161-176.
459

460 Singh, N., Turner, A., 2009. Trace metals in antifouling paint particles and their
461 heterogeneous contamination of coastal sediments. Marine Pollution Bulletin 58, 559-564.
462

463 Turner, A., Millward, G.E., 2002. Suspended particles: Their role in estuarine
464 biogeochemical cycles. Estuarine Coastal and Shelf Science 55, 857-883.
465

466 Turner, A., Rees, A., 2016. The environmental impacts and health hazards of abandoned
467 boats in estuaries. Regional Studies in Marine Science 6, 75-82.
468

469 Turner, A., Taylor, A., 2018. On site determination of trace metals in estuarine sediments by
470 field-portable-XRF. Talanta 190, 498-506.
471

472 Voparil, I.M., Burgess, R.M., Mayer, L.M., Tien, R., Cantwell, M.G., Ryba, S.A., 2004.
473 Digestive bioavailability to a deposit-feeder (*Arenicola marina*) of polycyclic aromatic

474 hydrocarbons associated with anthropogenic particles. *Environmental Toxicology and*
475 *Chemistry* 23, 2618-2626.
476